

Physical and Mechanical Characterization of Fiber Cell Wall in Castor (*Ricinus communis* L.) Stalk

Xiaoping Li,^{a,*} Guanben Du,^a Siqun Wang,^{b,*} and Guanxia Yu^c

Castor (*Ricinus communis* L.) stalk is a byproduct of the production of castor oil. As a natural material, castor stalk has great potential in the production of bio-composites as reinforcement materials. To provide more information about the castor stalk for using it better, the structure, microfibril angle (MFA), relative degree of crystallinity (%), and mechanical properties of castor fiber cell walls were investigated using X-ray diffraction (XRD) and nanoindentation. The influence of chemical composition and MFA on the mechanical properties of fiber cell wall was studied as well. The cortex of castor stalks primarily contains long fibers, while the xylem of castor stalk, an excellent wood-type material, comprises most of the castor stalk (83.95% by weight); the pith of the stalk is composed of parenchyma cells. The average elastic modulus of fiber cell wall in lower, upper, and branch parts are 16.0 GPa, 18.6 GPa, and 13.2 GPa, respectively. The average hardness of fiber cell wall in lower, upper, and branch parts are 0.50 GPa, 0.54 GPa, and 0.43 GPa, respectively. As lignin content increases from 15.57% to 17.41% and MFA decreases from 21.3° to 15.4°, the elastic modulus increases from 13.2 GPa to 18.6 GPa and the hardness increases from 0.43 GPa to 0.54 GPa. The mechanical properties, including the elastic modulus and the hardness of the fiber cell wall in the upper region of the castor stalk, are higher than those in the lower region, while the mechanical properties of the fiber cell wall in the branches are lower than those in either the upper or lower regions.

Keywords: Castor stalk; Fiber cell wall; Microfibril angle; Mechanical properties; Nanoindentation

Contact information: a: Yunnan Key Laboratory of Wood Adhesives and Glue Products, Southwest Forestry University, Kunming, 650224, PR China; b: Center for Renewable Carbons, University of Tennessee, Knoxville, TN, 37996, USA; c: College of Science, Nanjing Forestry University, Nanjing, 210037, PR China; * Corresponding authors: lxp810525@163.com; swang@utk.edu

INTRODUCTION

As the world's population has expanded and industry has rapidly developed, the need for energy has grown while natural resources have shrunk, as no significant new petroleum resources have been found. The resultant energy crisis has spawned the demand for renewable, natural fibers, and for bio-oil to replace oil-derived fibers and fuels (Mohan *et al.* 2006). In addition, with the rapid development of natural-fiber-based composites in recent years, more and more agricultural residues are being considered as sources for composites as reinforcement materials. These agricultural residues include hemp fiber (Sawpan *et al.* 2011), bamboo (Bhagat *et al.* 2013), flax (Ausias *et al.* 2013), and ramie (Li *et al.* 2013).

The castor plant (*Ricinus communis* L.) grows well in almost any environment, including saline alkali soils as well as in arid, hot, and cold climates. Castor has been planted widely in the world for thousands of years; castor oil pressed from the castor seed

is a unique vegetable oil containing high amounts (90%) of the hydroxy monounsaturated fatty acid ricinoleic acid. The oil can be used for the preparation of adhesives (Wechsler *et al.* 2013), biodiesel fuel (Mejía *et al.* 2013), feedstock for enzymatic production of methyl esters (Maleki *et al.* 2013), polyurethane (Yari *et al.* 2013), and polyols (Zhang *et al.* 2013). In short, castor oil is an important bio-renewable material that plays an important role, especially as petroleum resources dwindle.

The castor stalk is a byproduct of the production of castor seed, and its weight is 3 to 4 times that of the castor seed by weight. Finding productive uses for the castor stalk is very important in order to avoid waste in the production of castor oil. Recently, castor stalks have been used to prepare particleboard and fiberboard (Grigoriou and Ntalos 2001). But, to date, there has been little available information on the mechanical properties of fiber cell wall in castor stalk. The current research provides information on the physical and mechanical properties of castor stalk fiber cell wall through the use of nanoindentation. This study also provides a base of information about how to better use castor stalks in future.

Nanoindentation was first used by Wimmer *et al.* (1997) to study the mechanical properties of cell walls in wood materials, and it is currently used in wood science to study the mechanical properties of fiber cell walls in agricultural crop stalks (Wu *et al.* 2010), bamboo (Yu *et al.* 2007), hardwoods (Wu *et al.* 2009), and softwoods (Wimmer *et al.* 1997). The mechanical properties of hemp fiber and flax fiber along the fiber section were also measured by nanoindentation (Marrot *et al.* 2013; Bourmaud and Baley 2012). The research has shown that there are significant differences along the stem of biomass stalks, such as silvergrass (Liao *et al.* 2012), reed stalk (Wang *et al.* 2013), and hemp stalk core (Li *et al.* 2013b). However, little data utilizing nanoindentation have been gathered on castor stalk fibers.

The objective of this study was to investigate the mechanical properties (hardness [H] and elastic modulus [E]) of fiber cell wall along the length of the castor stalk stem. The influences of physical properties and chemical characteristics on the mechanical properties of the castor stalk fiber cell wall were also evaluated.

EXPERIMENTAL

Materials

The castor (*Ricinus communis* L.) stalk (Fig. 1A) used in this study was harvested in 2010 December, from Zibo, Shandong province, China, where the plant normally grows to about 3 to 5 m in height. It is an annual plant and measures between 10 and 50 mm in diameter with a hollow core. Castor stalks of this variety were oven-dried and stored in sealed plastic bags at 20 to 28 °C and a relative humidity of 40 to 60%. Three sampling areas were defined on one stem, as illustrated in Fig. 1B; the lower part was between 0 and 10 cm (The fiber bundle diameter was between 10 and 12 mm), the upper part was between 60 and 70 cm (The fiber bundle diameter was between 6 and 8 mm), and the branch parts were between 90 and 100 cm (The fiber bundle diameter was between 3 and 6 mm).

Measuring Biochemical Components

The cortex, xylem, and pith of castor stalk were separated by hand. The three group samples of different parts along the castor xylem stem were the lower part, upper

part, and branch part. The lignin content and holocellulose content were measured according to the China standard of “Fibrous raw material of sampling for analysis (GB/T 2677.1-1993)”. Lignin content was measured in the following way: Two copies 1g samples were extracted by benzyl alcohol solution. After the samples were dried in air, the samples were treated with 72% H_2SO_4 for 2.5 h in water at 18 to 20 °C. Then the treated samples were treated with 3% H_2SO_4 for 4 h in water at 100 °C. The residual mass was weighed, making it possible to calculate the lignin content; the difference between two copies should be less than 0.20%. Holocellulose content was measured in the following way: Two copies, 2 g samples, were extracted by benzyl alcohol solution, then treated by 65 mL distilled water with glacial acetic acid and sodium chlorite at 75 °C for 3 to 4 h until the samples were white. The residual mass was determined, followed by calculation of the holocellulose content, where the difference between two copies should be less than 0.40%.

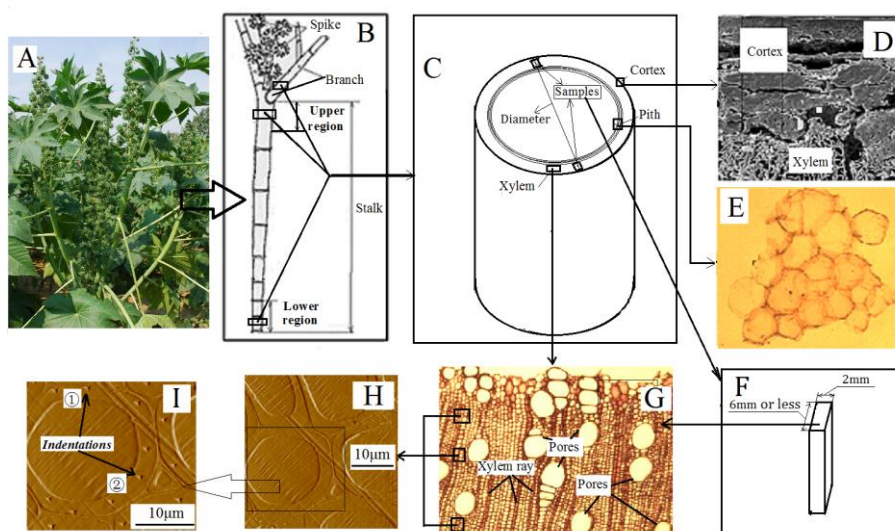


Fig. 1. Structure of the castor stalk. A. Castor plants; B. Three sampling areas from the castor stalk; C. Cross-section showing structure of castor stalk; D. The structure of the cortex in castor stalk; E. The structure of the pith in castor stalk; F. Sample for embedding used to nanoindentation; G. The structure of the xylem in castor stalk; H. The structure of castor stalk fiber cell wall; I. Indentations on fiber cell wall (① is invalid indentation, while ② is valid indentation).

Measuring Microfibril Angle (MFA) and Relative Degree of Crystallinity

To investigate the relationship between the microfibril angle, the relative degree of crystallinity, and the mechanical properties of cell walls in castor stalks, wide-angle X-ray diffraction analysis was conducted with a DX-200 materials research diffractometer (Dandong Fangyuan Instrument Co. Ltd., China) using a $Cu K\alpha$ radiation source. The size that was used for MFA testing was 1 mm thick X 15 mm long X 5 mm width, with 10 copies per sample from the midpoint location of the castor stalk. The method used for measuring the microfibril angle has been described in detail (Cave 1966). The MFA of the fiber wall layers was computed with Cave's (1966) formula (1) and the parameter T defined by Cave (1966) (shown in Fig. 2). The method of measuring the relative degree of crystallinity was as follows: the XRD pattern was recorded within an angle range of 2θ from 0 ° to 65 °, with a scanning rate of 0.05 °/s. Castor stalk “flour” (above 100 mesh) from three locations (lower part, higher part, and branch part, respectively) was prepared

by grinding the samples taken from the castor stalk stem. Discs with a diameter of 13 mm and a thickness of 1.6 mm were made by compressing 0.2 g of flour. The relative degree of crystallinity ($CrI\%$) was calculated based on the Segal method from the following equation (2) (Segal *et al.* 1959), with 6 to 8 copies per sample,

$$MFA=0.6T \quad (1)$$

where T was the X-ray diffraction parameter, MFA was the microfibril angle.

$$CrI\% = \frac{I_{002} - I_{am}}{I_{002}} \times 100 \quad (2)$$

In Eq. 2, the term I_{002} represents both the crystalline and amorphous parts, and I_{am} represents only the amorphous part.

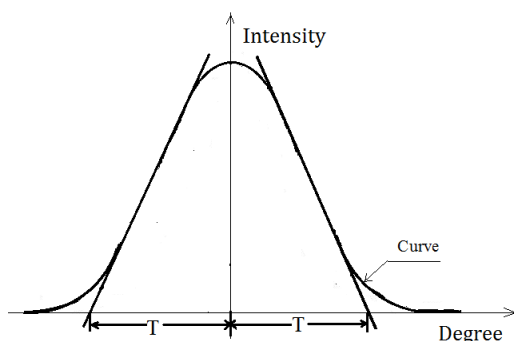


Fig. 2. Calculation method of microfibril angle

Nanoindentation

Three groups of samples from three locations at midpoint (two samples per location) were cut into small pieces of approximately 2 x 6 mm (or less than 6 mm) (as shown in Fig. 1F) after oven drying for the nanoindentation analysis. Each individual piece was glued onto chipboard and then put into a plastic mold. The chipboard, with a width equal to the diameter of the mold, was used to keep the samples in the correct orientation and to ensure that the axes of the fibers were parallel to the direction of nanoindentation. The embedding medium added into the plastic mold was epoxy resin, which was formulated with cycloaliphatic epoxide resin (ERL-4221) (2.5 parts), polycondieposide (DER-736) (1.5 parts), nonenyl succinic anhydride (NSA) (6.5 parts), and dimethylaminoethanol (DMAE) (0.1 parts) (Li *et al.* 2013); the molds were placed in an oven under vacuum for 30 to 40 min to remove any air and cured in the same oven at 70 °C for 8 to 10 h. The cured samples were trimmed to remove the epoxy resin and to expose the surface of the castor stalk. The surface was cut with a glass knife until the entire sample pieces had been cut. Finally, the top surface was smoothed with a diamond knife. The final specimens were put into a special container to protect the sample surfaces. All nanoindentation experiments were performed at the Center for Renewable Carbon using a TriboIndenter system. A Berkovich indenter, a three-sided pyramid with an area-to-depth function, which is the most commonly used in nanoindentation, was used for all experiments. Three to five locations per samples were tested by the Berkovich indenter, Two or three fibers were tested per location, for which the locations have to include the location closed to pith area, the location closed to cortex area, and the location in the

middle point between pith and cortex (Shown in Fig.1G). The indentation was performed in a displacement-controlled mode and consisted of three segments. In the first segment, loading force was applied at a constant displacement rate of 5 nm/s until the intended indentation depth of 200 nm was reached; the maximum force was kept at this depth for 10 s in the second segment and then unloaded at a constant displacement rate of 10 nm/s until 90% of the loading force was removed in the third segment (Fig. 3), in a process described in detail in Wu *et al.* (2009). Forty to sixty valid indentations were made on a cross-section of 10 to 15 cell walls for each group sample (Figs. 1H and 1I) (① is invalid indentation, while ② is valid indentation shown in Fig.1I). At the end, the hardness (H) and the elastic modulus (E) were calculated from the load-displacement data according to the method of Oliver and Pharr (1992). The results are shown in Table 1 and Fig.4.

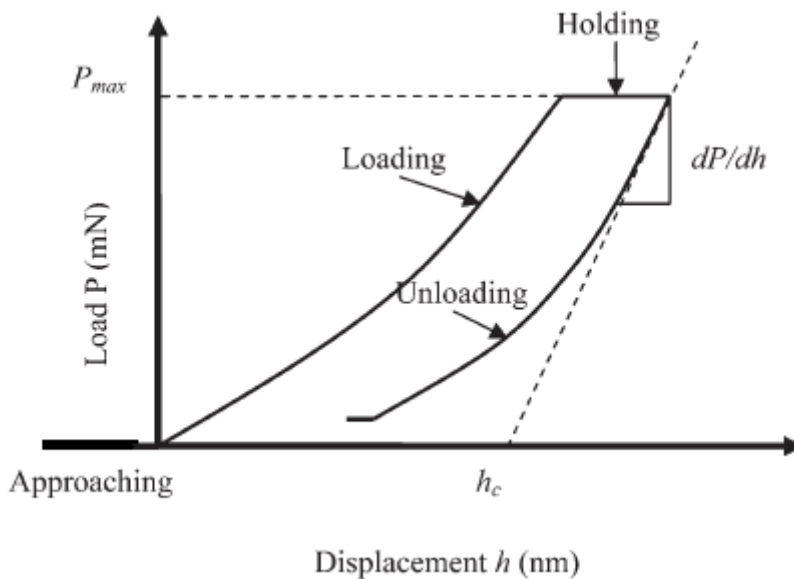


Fig. 3. Typical load displacement curve of a nanoindentation

RESULTS AND DISCUSSION

The Structure and Chemical Composition of the Castor Stalk

Castor stalk includes three parts: the cortex, the xylem, and the pith (as shown in Fig. 1C); their ratios were 10.90%, 83.95%, and 5.15%, respectively, by weight. The cortex contains long, strong fibers, and the longest fiber was 29.5 mm in length (shown in Fig. 1D). The lignin and holocellulose contents were 8.1% and 66.45%, respectively. The xylem looks structurally like hardwood (shown in Fig. 1G), and the fibers were 0.75 to 0.90 mm in length, 26.13 to 31.74 μm in diameter, and 4.38 to 5.8 μm in fiber cell wall thickness, while the lignin and holocellulose were 21.9% and 73.5%, respectively. The pith is primarily composed of parenchyma cells (shown in Fig. 1E), and the lignin and holocellulose were 8.77% and 70.5%, respectively. The pith can be used to prepare a biodegradable “green” foam used as an insulation material; its thermal conductivity is only 0.0539 W/m·K. In short, the xylem constitutes the greatest part of the castor stalk by weight; research into the mechanical properties of castor stalk fiber cell walls in the xylem will yield valuable information about how to use it more effectively.

Physical and Mechanical Properties of Fiber Cell Walls in the Castor Stalk

The MFA of the castor stalk are different in different regions of the stalk; the MFA is lower in the upper region, higher in the lower region, and highest in the branches (Table 1). The relative degree of crystallinity was found to decrease slightly from the bottom to the top of the castor stalk, and is almost identical in the upper region and branches (Table 1). The elastic modulus and hardness of the cell wall in the upper region of the castor stalk are higher than those in the lower region, with the lowest mechanical properties of cell walls in the branches.

The cell wall is composed of cellulose, hemicellulose, and lignin. These chemical composites are distributed in the different cell walls, including the primary wall (P) and the secondary walls (S1 layer, S2 layer, and S3 layer). The S2 layer is the thickest of all the cell wall layers. The spiral angle of the cellulose fibrils in this layer was measured in our experiment and is believed to be the most influential factor for the mechanical properties of single fibers (Page *et al.* 1977). The MFA is influenced by various factors, including the plant variety, the plant part (*i.e.*, early or late wood), and the growing environment of the plant (Lasserre *et al.* 2009). The MFA of three group samples taken from one stem of castor stalk were different, and the p values of the three parts were all smaller than 0.001 by paired t-test with SAS software. In other words, the difference was significant among the three parts. This is because all the samples were taken from one stem, but from different parts of the stem.

Table 1. Physical and Mechanical Properties of Fiber Cell Wall

| Sample Region | MFA (°) | Relative degree of crystallinity (%) | Elastic modulus (GPa) | Hardness (GPa) | Lignin content (%) |
|---------------|-------------|--------------------------------------|-----------------------|----------------|--------------------|
| Lower | 17.7 (0.05) | 43.6 (1.05) | 16.0 (1.92) | 0.50 (0.05) | 16.74 (0.09) |
| Upper | 15.4 (0.03) | 42.7 (0.98) | 18.6 (1.65) | 0.54 (0.04) | 17.41 (0.07) |
| Branch | 21.3 (0.06) | 42.6 (0.86) | 13.2 (1.36) | 0.43 (0.03) | 15.57 (0.08) |
| Mean | 18.2 (0.08) | 43.0 (1.25) | 15.9 (2.16) | 0.49 (0.06) | 16.57 (1.01) |

Note: standard deviations in parentheses

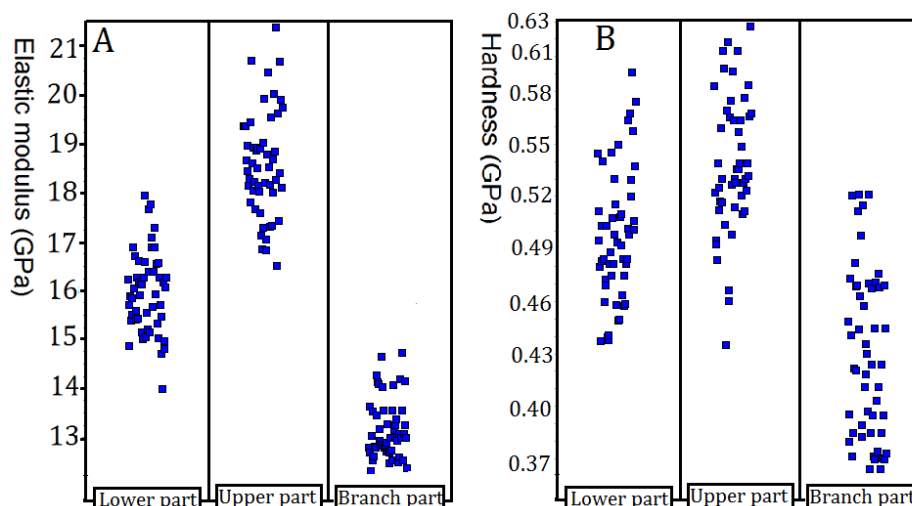


Fig. 4. The mechanical properties of fiber cell wall in different locations. A. The elastic modulus of fiber cell wall; B. The hardness of fiber cell wall

The mechanical properties of the fiber cell walls were affected by a number of factors, such as the density, MFA, chemical composite content (especially the lignin content) (Gindl *et al.* 2004; Tze *et al.* 2007), the type of plant (Wimmer *et al.* 1997; Wu *et al.* 2009; Wu *et al.* 2010), as well as other factors (Xing *et al.* 2008; Zhang *et al.* 2006). There was a negative correlation between the cell wall mechanical properties and the MFA (Gindl *et al.* 2004; Tze *et al.* 2007); as the cell-wall MFA increased, the mechanical properties (especially the elastic modulus) decreased. Similarly, the MFA in the branches was highest when the mechanical properties of the fiber cell wall in the branches were lowest (Fig. 4). So the results about the relationship between MFA and the mechanical properties of fiber cell wall were similar to the results in before research (Gindl *et al.* 2004; Tze *et al.* 2007).

Chemical composition can also affect the mechanical properties of castor stalk fiber cell walls. As lignin content increases, so do the mechanical properties of the cell wall, especially the hardness (Konnerth *et al.* 2009). In different regions of the castor stalk, the lignin content of castor stalk in the upper region was higher compared to the lower region and branches. The trend held with regard to the mechanical properties and the lignin content in different locations of the castor stalk. So the relationship between the lignin content and the elastic modulus and hardness was a positive correlation.

The results of the present study were similar to those of other studies (Gindl *et al.* 2004; Tze *et al.* 2007). As the MFA decreased or the lignin content increased in three different regions of the castor stalk, the mechanical properties of fiber cell wall increased. The mechanical properties of the fiber cell wall in the upper region were higher than those in the lower region; this result is similar to the results of Liao *et al.* (2012) and Wang *et al.* (2013).

CONCLUSIONS

The physical, chemical characteristics, and mechanical properties of fiber cell wall in xylem part of castor stalk were investigated and the conclusions were drawn as followed.

1. Castor stalk includes three parts: the cortex, the xylem, and the pith, respectively. The cortex contains long fibers, and the longest fiber was 29.5 mm in length. The pith is primarily composed of parenchyma cells and it can be used to prepare a biodegradable “green” foam used as an insulation material; its thermal conductivity is only 0.0539 W/m·K.
2. The xylem looks structurally like hardwood and it constitutes the greatest part of castor stalk (83.95% of the stalk by weight). The fibers in the xylem part were 0.75 to 0.90 mm in length, 26.13 to 31.74 μm in diameter, and 4.38 to 5.8 μm in fiber cell wall thickness, while the lignin, cellulose, and hemicellulose contents were 16.74%, 33.8%, and 13.43%, respectively.
3. The MFA, relative degree of crystallinity, lignin content, elastic modulus, and hardness of fiber cell walls in the xylem part of castor stalk were 18.2°, 43.0%, 16.74%, 15.9 GPa, and 0.49 GPa, respectively. These results were all different in different parts along the stem of castor stalk.

- The mechanical properties of the fiber cell walls in the upper region of the stalk were higher than those of the fiber cell walls in the lower region because the MFA of the fiber cell walls was smaller and the lignin content higher in the upper region than the MFA and the lignin content in the lower region. In addition, the mechanical properties of fiber cell walls in the branches were the lowest.

ACKNOWLEDGMENTS

The authors are grateful for the support of the Yunnan Province Nature Science Foundation (No. 2010CD064) and the National Nature Science Foundation (No. 30928022 and No. 31200437). The authors also thank Dr. Omid Hosseinaei at the Center for Renewable Carbon, University of Tennessee, Knoxville, TN, for assisting with the research.

REFERENCES CITED

- Ausias, G., Bourmaud, A., Coroller, G., and Baley, C. (2013). "Study of the fibre morphology stability in polypropylene-flax composites," *Polymer Degradation and Stability* 98(6), 1216-1224.
- Bourmaud, A., and Baley, C. (2012). "Nanoindentation contribution to mechanical characterization of vegetal fibers," *Composites Part B: Engineering* 43(7), 2861-2866.
- Bhagat, D., Gupta, M., and Bhalla, S. (2013). "Design and strength analysis of composite bamboo column elements," *IOSR Journal of Engineering* 3(6), 31-36.
- Cave, I. D. (1966). "Theory of X-ray measurement of microfibril angle in wood," *Forest Products Journal* 16(10), 37-42.
- Grigoriou, A. H., and Ntalos, G. A. (2001). "The potential use of *Ricinus communis* L. (castor) stalks as a lignocellulosic resource for particleboards," *Industrial Crops and Products* 13(3), 209-218.
- Gindl, W., Gupta, H. S., Schoberl, T., Lichtenegger, H. C., and Fratzl, P. (2004). "Mechanical properties of spruce wood cell walls by nanoindentation," *Applied Physics A-Materials Science & Processing* 79(8), 2069-2073.
- Konnerth, J., Gierlinger, N., Keckes, J., and Gindl, W. (2009). "Actual versus apparent within cell wall variability of nanoindentation results from wood cell walls related to cellulose microfibril angle," *Journal of Materials Science* 44(16), 4399-4406.
- Lasserre, J. P., Mason, E. G., Watt, M. S., and Moore, J. R. (2009). "Influence of initial planting spacing and genotype on microfibril angle, wood density, fibre properties and modulus of elasticity in *Pinus radiata* D. Don corewood," *Forest Ecology and Management* 58(9), 1924-1931.
- Liao, C., Deng, Y., Wang, S., Meng, Y., Wang, X., and Wang, N. (2012). "Microstructure and mechanical properties of silvergrass fibers cell evaluated by nanoindentation," *Wood and Fiber Science* 44(17), 63-70.
- Li, Y., Moyo S., Ding, Z., Shan, Z., and Qiu, Y. (2013). "Helium plasma treatment of ethanol-pretreated ramie fabrics for improving the mechanical properties of ramie/polypropylene composites," *Industrial Crops and Products* 51, 299-305.

- Li, X., Wang, S., Du, G., Wu, Z., and Meng, Y. (2013). "Variation in physical and mechanical properties of hemp stalk fibers along height of stem," *Industrial Crops and Products* 42, 344-348.
- Marrot, L., Lefeuvre, A., Pontoire, B., Bourmaud, A., Baley, C. (2013). "Analysis of the hemp fiber mechanical properties and their scattering (Fedora 17)," *Industrial Crops and Products* 51, 317-327.
- Mohan, D., Pittman, C. U., and Steele, P. H. (2006). "Pyrolysis of wood/biomass for bio-oil: A critical review," *Energy & Fuels* 20(3), 848-889.
- Maleki, E., Aroua, M. K., and Sulaiman, N. M. N. (2013). "Castor oil - A more suitable feedstock for enzymatic production of methyl esters," *Fuel Processing Technology* 112, 129-132.
- Mejía, J. D., Salgado, N., and Orrego, C. E. (2013). "Effect of blends of diesel and palm-castor biodiesels on viscosity, cloud point and flash point," *Industrial Crops and Products* 43, 791-797.
- Oliver, W. C., and Pharr, G. M. (1992). "An improved technique for determining hardness and elastic modulus using load and displacement sensing indentation experiments," *Journal of Materials Research* 7(6), 1564-1583.
- Page, D. H., Elhosseiny, F., Winkler, K., and Lancaster, A. P. S. (1977). "Elastic-modulus of single wood pulp fibers," *TAPPI J.* 60(4), 114-117.
- Segal, L., Creely, J., Martin, A., and Conrad, C. (1959). "An empirical method for estimating the degree of crystallinity of native cellulose using the X-ray diffractometer," *Textile Research Journal* 29(10), 786-794.
- Sawpan, M. A., Pickering, K. L., and Fernyhough, A. (2011). "Improvement of mechanical performance of industrial hemp fibre reinforced polylactide biocomposites," *Composites Part A-Applied Science and Manufacturing* 42(3), 310-319.
- Tze, W. T. Y., Wang, S., Rials, T. G., Pharr, G. M., and Kelley, S. S. (2007). "Nanoindentation of wood cell walls: Continuous stiffness and hardness measurements," *Composites Part A-Applied Science and Manufacturing* 38(3), 945-953.
- Wimmer, R., Lucas, B. N., Tsui, T. Y., and Oliver, W. C. (1997). "Longitudinal hardness and Young's modulus of spruce tracheid secondary walls using nanoindentation technique," *Wood Science and Technology* 31(2), 131-141.
- Wu, Y., Wang, S., Zhou, D., Xing, C., and Zhang, Y. (2009). "Use of nanoindentation and Silviscan to determine the mechanical properties of 10 hardwood species," *Wood and Fiber Science* 41(1), 64-73.
- Wu, Y., Wang, S., Zhou, D., Xing, C., Zhang, Y., and Cai, Z. (2010). "Evaluation of elastic modulus and hardness of crop stalks cell walls by nano-indentation," *Bioresource Technology* 101(8), 2867-2871.
- Wang, X., Deng, Y., Wang, S., Liao, C., Meng, Y., and Pham, T. (2013). "Nanoscale characterization of reed stalk fiber cell walls," *BioResources* 8(2), 1986-1996.
- Wechsler, A., Zaharia, M., Crosky, A., Jones, H., Ramírez, M., Ballerini, A., Nuñez, M., and Sahajwalla, V. (2013). "Macadamia (*Macadamia integrifolia*) shell and castor (*Ricinus communis*) oil based sustainable particleboard: A comparison of its properties with conventional wood based particleboard," *Materials and Design* 50, 117-123.

- Xing, C., Wang, S., Pharr, G. M., and Groom, L. H. (2008). "Effect off thermo-mechanical refining pressure on the properties of wood fibers as measured by nano-indentation and atomic force microscopy," *Holzforschung* 62(2), 230-236.
- Yu, Y., Fei, B., Zhang, B., and Yu, X. (2007). "Cell-wall mechanical properties of bamboo investigated by in-situ imaging nano-indentation," *Wood and Fiber Science* 39(4), 527-535.
- Yu, Y., Fei, B., Wang, H., and Tian, G. (2010). "Longitudinal mechanical properties of cell wall of Masson pine (*Pinus massoniana* Lamb) as related to moisture content: A nanoindentation study," *Holzforschung* 65(1), 121-126.
- Yari, A., Yeganeh, H., Bakhshi, H., and Gharibi, R. (2013). "Preparation and characterization of novel antibacterial castor oil-based polyurethane membranes for wound dressing application," *Journal of Biomedical Materials Research Part A* 102(1), 84-96.
- Zhang, Y., Zhang, S., Chui, Y., and Wan, H. (2006). "Effect of impregnation and in-situ polymerization of methacrylates on hardness of sugar maple wood," *Journal of Applied Polymer Science* 99(4), 1674-1683.
- Zhang, C., Xia, Y., Chen, R., Huh, S., Johnston, P. A., and Kessler, M. R. (2013). "Soy-castor oil based polyols prepared using a solvent-free and catalyst-free method and polyurethanes therefrom," *Green Chemistry* 15(6), 1477-1484.

Article submitted: November 21, 2013; Peer review completed: January 9, 2014; Revised version received and accepted: January 30, 2014; Published: February 3, 2014.